Pulse Delay and Advancement in SOI Microring Resonators With Mutual Mode Coupling

Tao Wang, *Student Member, IEEE*, Fangfei Liu, *Student Member, IEEE*, Jing Wang, Yue Tian, *Student Member, IEEE*, Ziyang Zhang, Tong Ye, Min Qiu, *Member, IEEE*, and Yikai Su, *Senior Member, IEEE*

***Abstract*—In this paper, we experimentally demonstrate continuously tunable pulse propagation in SOI microring resonators with mutual mode coupling, which is induced by nanosized gratings along the ring sidewalls. In the presence of the mutual mode coupling, dispersion-induced group delay is investigated in single-waveguide and double-waveguide coupled single-ring resonators, respectively. In particular, pulse propagation in the drop channel of a double-waveguide coupled resonator is observed and exhibits continuously tunable delay and advancement features in the experiment. Delayed pulses are also obtained at the reflection port of a single-waveguide coupled resonator due to the existence of backward whispering gallery mode (WGM).**

***Index Terms*—Group delay, microring resonator, pulse propagation, silicon photonics.**

I. Introduction

TUNABILITY of light velocity has become an important topic in the field of optics. It may be applied to all optical packet switched networks [1], optical interconnects in computer systems to avoid traffic contention [2], and true time delay for synthetic aperture radars [3]. Slow and fast light can be achieved by launching the light through media with positive and negative group delays, respectively. Experimental demonstrations of slow and fast light have been realized based on stimulated Brillouin scattering in optical fibers [4], four wave mixing processes in semiconductor optical amplifier (SOA) [5], electromagnetically induced absorption and transparency (EIA and EIT) in atomic vapors [6], [7], and structural dispersion in microsphere-optical fiber systems [8].

Manuscript received March 05, 2009; revised June 02, 2009. First published July 07, 2009; current version published September 10, 2009. This work was supported in part by the NSFC under Grant 60777040, in part by the Shanghai Rising Star Program Phase II under Grant 07QH14008, and in part by the 863 High-Tech Program under Grant 2009AA01Z257. The work of Z. Zhang and M. Qiu was supported in part by the Swedish Foundation for Strategic Research (SSF) through the Future Research Leader Program and in part by the Swedish Research Council (VR).

T. Wang, F. Liu, T. Ye, and Y. Su are with the State Key Laboratory of Advanced Optical Communication Systems and Networks, Department of Electronic Engineering, Shanghai Jiao Tong University, Shanghai 200240, China (e-mail: wangtao2007@sjtu.edu.cn; lfflys@sjtu.edu.cn; yetong@sjtu.edu.cn; yikaisu@sjtu.edu.cn).

J. Wang, Z. Zhang, and M. Qiu are with the Department of Microelectronics and AppliedPhysics, Royal Institute of Technology (KTH), 164 40 Kista, Sweden (e-mail: wangj@kth.se; zzy4680@yahoo.co.uk; min@kth.se).

Color versions of one or more of the figures in this paper are available online at http://ieeexplore.ieee.org.

Digital Object Identifier 10.1109/JLT.2009.2026590

Recently, silicon-on-insulator (SOI) platform shows attractive advantages for highly compact photonic devices due to its high refractive-index contrast between the silicon core and silica cladding. The fabrication process can be readily borrowed from electronics industry. Optical delay lines based on SOI microring resonators were investigated and their high efficiency to perform slow light function was well received [9]. Superluminal pulse propagation was also observed in a resonance-split single-waveguide coupled resonator [10] and in a structure consisting of two microrings [11]. Lately, we have shown the tunability from fast to slow light in a microring resonator with preliminary investigations [12]. In this paper, we report, for the first time, that the mutual mode coupling leads to some special features in the transmission and group delay variations at the reflection port of single-waveguide coupled resonators, and at the drop and add port of double-waveguide coupled resonators, respectively. For the double-waveguide coupled resonators, it turns out that slow light can be collected at the add port as the sidewall gratings reflect a certain amount of optical power into the backward whispering gallery mode (WGM) [13], and the delay time can be tuned in a certain wavelength range with little transmission variation. Moreover, it is theoretically found that both the positive and negative group delay can be achieved in the drop channel of the resonator and continuously-tunable slow- to fast- light is experimentally demonstrated by shifting the resonances through thermal heating of the device using a control light. With a continuous-wave (CW) optical input, the thermal nonlinear effect can dominate over carrier nonlinear effect with proper device size, and the effect possesses the lowest power requirement compared to other optical nonlinearity based tuning mechanisms [14], [15]. For the single-waveguide coupled resonators, pulse propagation shows similar characteristics to the case at the add port of double-waveguide coupled resonators and delay pulses are experimentally observed at the reflection port.

In Section II, the structure of microring sidewall gratings is illustrated as well as its induced counter-propagating mutual mode coupling; in Section III, we theoretically analyze transmission and group delay variation of single-waveguide and double-waveguide coupled resonators, respectively; in Section IV, we show the experimental results, including the measured transmission spectra and output pulse waveforms, which are delayed/advanced in different channels of the resonators.

II. Sidewall Grating Induced Mutual Mode Coupling

In microring resonators on the SOI platform, the sidewall gratings along the ring are previously considered as a result of

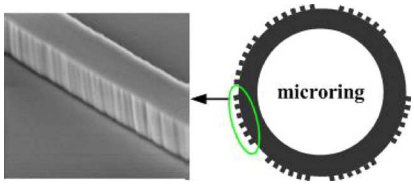

Fig. 1. SEM photograph and schematic of the quasi-gratings along the sidewall of the microring resonator.

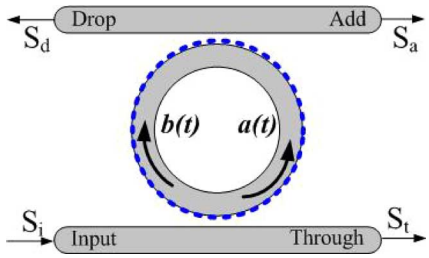

Fig. 2. Schematic of the double-waveguide coupled resonator with mutual mode coupling.

fabrication imperfection and not desirable in some applications, such as filtering and modulating. However, many important functions relying on the grating-assisted counter-directional mutual mode coupling were reported lately, such as dense wavelength conversion and multicasting [16], format conversion from non-return-zero (NRZ) to frequency shift keying (FSK) [17], and optical up-conversion in radio over fiber systems [18].

Fig. 1 shows the scanning electron microscope (SEM) photos of the sidewall gratings. These rectangular gratings resemble a group of ridges, which appear to have similar amplitude and period. This traces back to the fabrication process. During the electron beam lithography (Raith 150, 25 kV), a circular exposure line is actually broken down into a closed polygene path, forming edges and corners in the micro-ring structure. Along each edge, there are a limited number of actual exposure dots with the same step size. Together with the limited material resolution of the negative resist (maN2405), some 30–50 nm ridges are formed in a semi-periodic manner along the microring sidewalls. Based on the SEM photos and the understanding of the fabrication process, we treat the sidewall ridges analogous to several rectangular corrugated gratings with the same size and period, only separated with different distances. By setting up the number of the vertices (corners) of the polygons, the E-beam scan step size, and the exposure dose, the period and amplitude of the gratings can be tuned [19]. During the characterization of the ring-resonators and data analysis, small-step changes in the scanning pattern play a major role in altering the mutual coupling while the scattering loss is not much affected. As a result, backward WGM is accumulated and generated due to the perturbation provided by the gratings. To better describe the mutual mode coupling between the forward and backward WGM, we define a mutual coupling quality factor Q_μ [19], which is determined by the reflectivity of the gratings.

III. Transmission and Group Delay Variation

Here, we investigate the transmission and group delay variation for both the single-waveguide and double-waveguide coupled microring resonators with mutual mode coupling using the coupled mode theory.

A. Double-Waveguide Coupled Resonators

The structures of the double-waveguide coupled microring resonators are depicted in Fig. 2. As discussed in [19], an incident wave S_i generates a counter-clockwise traveling mode $\boldsymbol{a(t)}$, which in turn induces a counter-propagation mode $\boldsymbol{b(t)}$ due to periodic structural roughness along the sidewall of the microring. These two travelling modes are related by the mutual coupling factor $\mathrm{Q_u}$.

To simplify the analysis, we assume that modes $\boldsymbol{a}$ and $\boldsymbol{b}$ have the same resonance frequency ω_0, and intrinsic quality factor Q_i. Coupling quality factors Q_{e1} and Q_{e2} are defined corresponding to the ring coupled to the lower and upper waveguides, respectively. Similar to [20], the transfer functions of the through channel $\mathrm{T}(\delta)$, drop channel $\mathrm{D}(\delta)$, and add channel $\mathrm{A}(\delta)$ are as follows, respectively:

$$T(\delta)=\frac{S_t}{S_i}=1-\frac{1}{2Q_{e1}}\left[\frac{1}{j\left(\delta+\frac{1}{2Q_\mu}\right)+\frac{1}{2Q_i}+\frac{1}{2Q_{e1}}+\frac{1}{2Q_{e2}}}+\frac{1}{j\left(\delta-\frac{1}{2Q_\mu}\right)+\frac{1}{2Q_i}+\frac{1}{2Q_{e1}}+\frac{1}{2Q_{e2}}}\right] \tag{1}$$

$$D(\delta)=\frac{S_d}{S_i}=\frac{1}{2}\sqrt{\frac{1}{Q_{e1}Q_{e2}}}\left[\frac{1}{j\left(\delta+\frac{1}{2Q_\mu}\right)+\frac{1}{2Q_i}+\frac{1}{2Q_{e1}}+\frac{1}{2Q_{e2}}}+\frac{1}{j\left(\delta-\frac{1}{2Q_\mu}\right)+\frac{1}{2Q_i}+\frac{1}{2Q_{e1}}+\frac{1}{2Q_{e2}}}\right] \tag{2}$$

$$A(\delta)=\frac{S_a}{S_i}=\frac{1}{2}\sqrt{\frac{1}{Q_{e1}Q_{e2}}}\left[\frac{1}{j\left(\delta+\frac{1}{2Q_\mu}\right)+\frac{1}{2Q_i}+\frac{1}{2Q_{e1}}+\frac{1}{2Q_{e2}}}-\frac{1}{j\left(\delta-\frac{1}{2Q_\mu}\right)+\frac{1}{2Q_i}+\frac{1}{2Q_{e1}}+\frac{1}{2Q_{e2}}}\right] \tag{3}$$

where $\delta=(\omega-\omega_0)/\omega_0$ denotes the normalized frequency detuning. It can be seen from the above equations that the traveling mode is split into two sub-resonance frequencies, i.e., $\delta+1/2\mathrm{Q}_\mu$ and $\delta-1/2\mathrm{Q}_\mu$. Therefore, the splitting separation is solely determined by the value of Q_μ. For $\mathrm{Q}_\mu\rightarrow\infty$, (1)–(2) reduces to a conventional single-ring without mutual-coupling case and $\mathrm{A}(\delta)=0$ is obtained as no light comes from the add port. We define an optimal mutual coupling quality factor $\mathrm{Q_m}$ satisfying $1/Q_{\mathrm{m}}^2=|1/Q_{e1}^2-(1/Q_i+1/Q_{e2})^2|$. $\mathrm{Q_m}$ can be considered as a critical coupling parameter since the input optical signal is

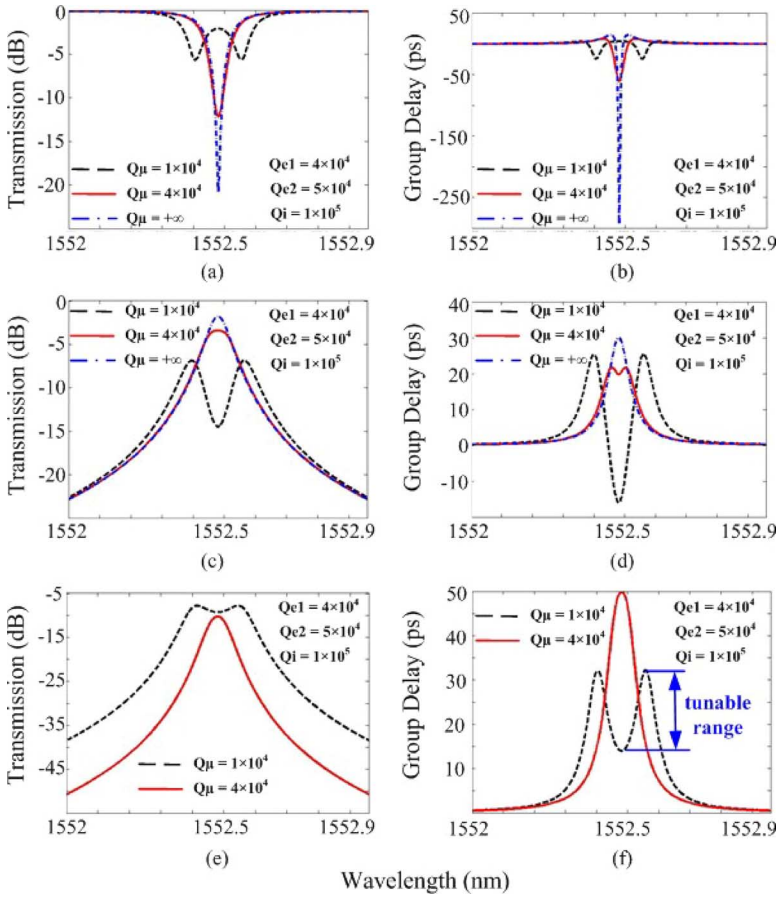

Fig. 3. Transmissions and corresponding group delays in the through (a-b), drop (c-d), and add (e-f) channels, respectively with $1/\mathrm{Qe}_1 < (1/\mathrm{Q}_i + 1/\mathrm{Q}_{e2})$.

completely removed from the through channel ideally. Based on the analysis in [21], the effective phase shifts for the three channels are defined as $\Phi_t = \arg(\mathrm{T}(\delta))$, $\Phi_d = \arg(\mathrm{D}(\delta))$, and $\Phi_a = \arg(\mathrm{A}(\delta))$, respectively, and the derived dispersion-induced group delays are given by

$$\tau_{t,d,a}(\delta) = -\frac{d\Phi_{t,d,a}(\delta)}{d\delta}. \tag{4}$$

It implies that pulses will be delayed/advanced through this system when the corresponding group delay has a positive/negative value, respectively.

Fig. 3 depicts the normalized transmission and group delay for the under-coupling case, i.e., $1/\mathrm{Qe}_1 < (1/\mathrm{Q}_i + 1/\mathrm{Qe}_2)$ [22]. $\mathrm{Q}_\mu \to \infty$ corresponds to the case of an under-coupled ring resonator without mutual-coupling. In the through channel, Fig. 3(a) shows that the mutual-coupling lowers the resonance notch depth in the transmission with the decreasing of Q_μ, which leads to anomalous dispersion in the case of $\mathrm{Q}_\mu > \mathrm{Q}_\mathrm{m}$,, as shown in Fig. 3(b). When $\mathrm{Q}_\mu < \mathrm{Q}_\mathrm{m}$, resonance-splitting takes place. Anomalous dispersion, and, thus, fast light can be observed at the split resonances. In the drop channel, the decreasing of Q_μ lowers the dropped optical power and induces normal dispersion, shown in Fig. 3(c) and (d). Similar to the case in the through port, resonance splitting appears when $\mathrm{Q}_\mu < \mathrm{Q}_\mathrm{m}$ and enhanced with the decreasing of Q_μ. As a result, normal dispersion exists on each split resonance. Moreover, anomalous dispersion exhibits between the split resonances, implying that continuously-tunable slow- to fast light can be obtained across the split resonances. At the "add" port, no light comes out if $\mathrm{Q}_\mu \to \infty$ due to the absence of the backward mode. As shown in Fig. 3(e), the transmission increases and resonance-splitting appears as the value of Q_μ becomes smaller, indicating emergence of the backward optical power. When $\mathrm{Q}_\mu < \mathrm{Q}_\mathrm{m}$, positive group delay can be achieved around the split resonances and the delay can be tuned if signals shift from either of the split resonances to the central wavelength, which is illustrated in Fig. 3(f). The tunable range is defined as the difference between maximal delay obtained on the split resonances and that achieved at the center wavelength. However, group delay is tuned in company with transmission variation, which is defined as the difference between transmission on the split resonances and that at the central wavelength among the split resonances. Larger tunable range can be obtained at the cost of larger transmission variation.

Fig. 4 displays the over-coupling case, i.e., $1/\mathrm{Qe}_1 > (1/\mathrm{Q}_i + 1/\mathrm{Qe}_2)$. Normal dispersion and correspondingly slow light can be achieved without mutual-coupling at the through port, as shown in Fig. 4(b). As the mutual-coupling increases (Q_μ decreases from $+\infty$), Fig. 4(a) shows that the mutual-coupling enhances the resonance notch depth and has little impact on the group delay if $\mathrm{Q}_\mu > \mathrm{Q}_\mathrm{m}$. At $\mathrm{Q}_\mu = \mathrm{Q}_\mathrm{m}$, the transmission is zero at resonance. However, once the mutual-coupling further increases ($\mathrm{Q}_\mu < \mathrm{Q}_\mathrm{m}$), resonance-splitting takes place and negative group delay can be obtained at the split resonances. For the

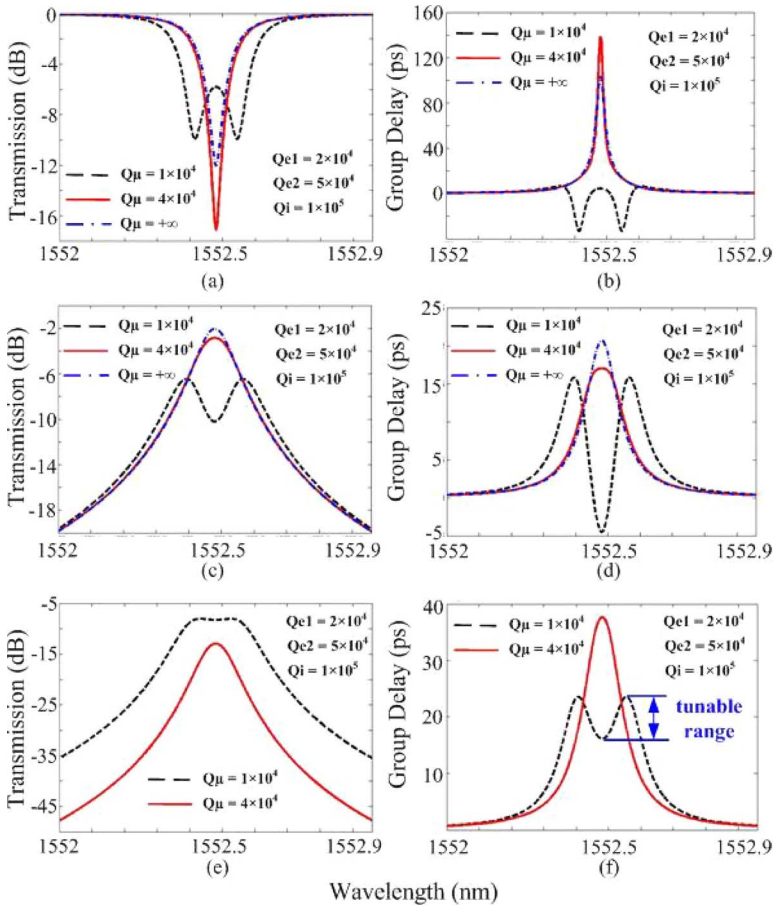

Fig. 4. Transmissions and corresponding group delays in the through (a-b), drop (c-d), and add (e-f) channels, respectively with $1/\mathrm{Q}_{e1} > (1/\mathrm{Q}_i + 1/\mathrm{Q}_{e2})$.

drop and add channels, the characteristics of transmission and group delay are in accordance with that in the under-coupling case, though the maximal delay time reduces as well as the tunable range across the split resonances due to the decreasing of Q_{e1}, as shown in Fig. 4(c)–(f).

Despite the facts that group delay properties have already been studied before [22], [23], there are some new features in the drop and add channels by the nature of the mutual mode coupling. Normal and anomalous dispersions appear simultaneously around the split resonances, leading to larger tunable range at the drop port. Slow light tuning with minor optical power variation can be achieved at the add port. Thus, the mutual-coupling offers another degree of freedom when performing slow-light and fast-light functions.

B. Single-Waveguide Coupled Resonators

In previous works [10], group delay was investigated and fast light was experimentally demonstrated in the through channel. However, the characteristics of backward optical signals reflected by the sidewall gratings have not been reported in SOI microring resonators.

Fig. 5 depicts the schematic of a single-waveguide coupled resonator. Similar to the analysis for double-waveguide coupled resonators, the transfer function of the through and reflection port can be respectively expressed as follows:

$$T(\delta) = \frac{S_t}{S_i} = 1 - \frac{1}{2Q_e}\left[\frac{1}{j\left(\delta + \frac{1}{2Q_\mu}\right) + \frac{1}{2Q_i} + \frac{1}{2Q_e}} + \frac{1}{j\left(\delta - \frac{1}{2Q_\mu}\right) + \frac{1}{2Q_i} + \frac{1}{2Q_e}}\right] \tag{5}$$

$$R(\delta) = \frac{S_r}{S_i} = \frac{1}{2}\frac{1}{Q_e}\left[\frac{1}{j\left(\delta + \frac{1}{2Q_\mu}\right) + \frac{1}{2Q_i} + \frac{1}{2Q_e}} - \frac{1}{j\left(\delta - \frac{1}{2Q_\mu}\right) + \frac{1}{2Q_i} + \frac{1}{2Q_e}}\right] \tag{6}$$

where $\delta = (\omega - \omega_0)/\omega_0$ denotes the normalized frequency detuning. Q_i and Q_e represent intrinsic quality factor and coupling quality factor, respectively. The mutual coupling factor Q_μ is also defined to indicate the coupling strength. Critical coupling is achieved if $1/Q_{\mathrm{m}}^2 = |1/Q_e^2 - 1/Q_i^2|$ is satisfied. The effective phase shifts for the two channels are defined as $\Phi_t = \arg(\mathrm{T}(\delta))$,

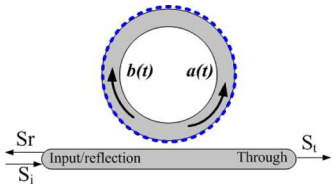

Fig. 5. Schematic of the single-waveguide coupled resonators with mutual mode coupling.

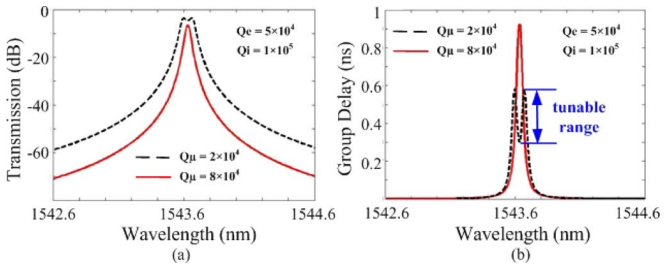

Fig. 6. (a) Transmission and (b) corresponding group delay at the reflection port with different Q_{u}.

$\Phi_r = \arg(\mathrm{R}(\delta))$, respectively, and the derived dispersion-induced group delays are given by

$$\tau_{t,r}(\delta) = -\frac{d\Phi_{t,r}(\delta)}{d\delta}. \tag{7}$$

Here, we focus on the transmission and group delay at the reflection port of single-waveguide coupled resonators.

Fig. 6 presents the transmission and group delay for the cases of $\mathrm{Q}_\mu < \mathrm{Q}_\mathrm{m}$ and $\mathrm{Q}_\mu > \mathrm{Q}_\mathrm{m}$, respectively. Their features seem similar to those obtained at the add port of double-waveguide coupled resonators. However, both the maximal delay time and tunable range are enhanced with the same Q_i and Q_e.

Since large tunable range with constant output power are desired in practical applications such as photonic RF phase shifters [24], it is important to investigate the relation between the tunable range of group delay and the optical power variation around the resonances. Fig. 7 shows the calculated results with different Q_i and Q_e. Initially, we plot transmission variation $\Delta\mathrm{P}$, maximal delay $\tau_{\max}$, and tunable range $\Delta\tau$ as functions of Q_i with $\mathrm{Q}_e = 2 \times 10^4$. Both $\tau_{\max}$ and $\Delta\tau$ increase with Q_i increasing. However, the rate decreases rapidly when Q_i goes up to 1×10^5. Meanwhile, $\Delta\mathrm{P}$ is limited to 1 dB. Furthermore, we investigate the transmission and group delay with larger Q_e, as shown in Fig. 7(b) and (c). $\tau_{\max}$ and $\Delta\tau$ increase significantly when Q_e becomes higher. However, the transmissions in these two cases show larger variations. Therefore, tradeoffs between the delay and optical power variation should be made according to different requirements in practical systems.

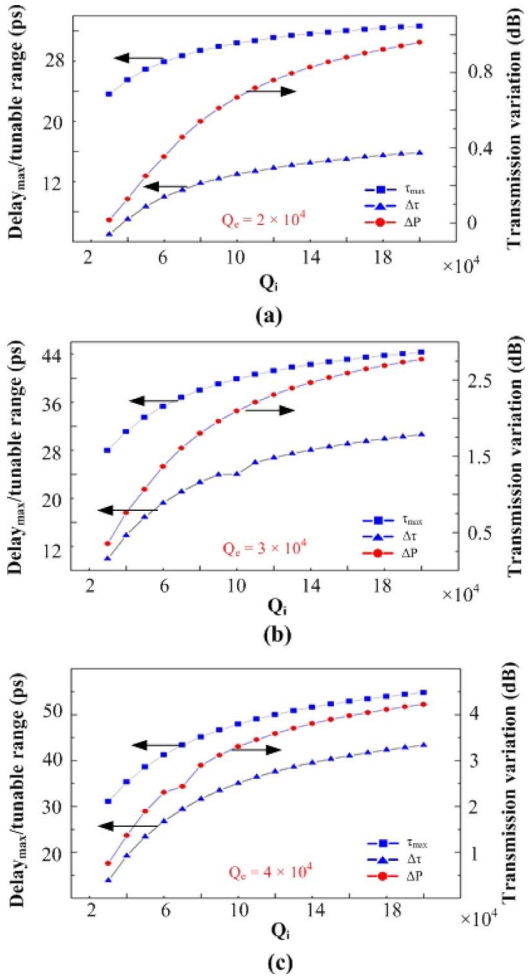

Fig. 7. Maximal group delay $\tau_{\max}$, tunable range $\Delta\tau$, and transmission variation $\Delta\mathrm{P}$ as functions of Q_i with (a) $\mathrm{Q}_e = 2 \times 10^4$, (b) $\mathrm{Q}_e = 2 \times 10^4$, and (c) $\mathrm{Q}_e = 4 \times 10^4$, respectively.

IV. Experiments and Results

A. Characterization of Microring Resonators

The resonators used in the experiments are fabricated on a commercial single-crystalline SOI wafer with a 250-nm-thick silicon slab on top of a 3-μm silica buffer layer. The cross section of the silicon waveguide is 450×250 nm^2 with an effective area of 0.1 μm^2 for the transverse-electric (TE) mode. The scanning electron microscope (SEM) photographs of the double-waveguide and single-waveguide coupled resonators are shown in Fig. 8. The microring with a radius of 20 μm is sandwiched between two straight waveguides in the double-waveguide coupled resonator and side coupled to one straight waveguide in the single-waveguide coupled resonator, respectively, with an air gap of 120 nm. The device is fabricated by E-beam lithography followed by reactive ion etching. The waveguide propagation loss is ~ 2.8 dB/cm by using the method in [25].The straight waveguide is carefully tapered to a width of 10 μm at both ends, where gold grating couplers are added to couple light near vertically from single mode fibers. The grating coupler supports only TE mode with a fiber-to-fiber loss of ~ 20 dB, which would be reduced by optimizing the individual teeth and slit widths of the gold gratings [26].

Fig. 9(a) presents the spectral response measured at the through and drop ports of the double-waveguide coupled resonator around a wavelength at 1552.48 nm. The spectral responses are fitted using (1) and (2). Since the straight waveguides are symmetrically coupled to the microring, i.e., $\mathrm{Q}_e \approx \mathrm{Q}_{e1}$, the obtained intrinsic Q_i and coupling $\mathrm{Q}_e(\mathrm{Q}_{e1})$

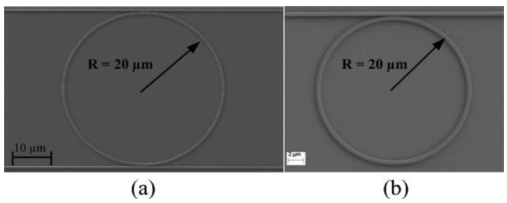

Fig. 8. SEM photographs of the (a) double and (b) single-waveguide coupled resonators with mutual mode coupling.

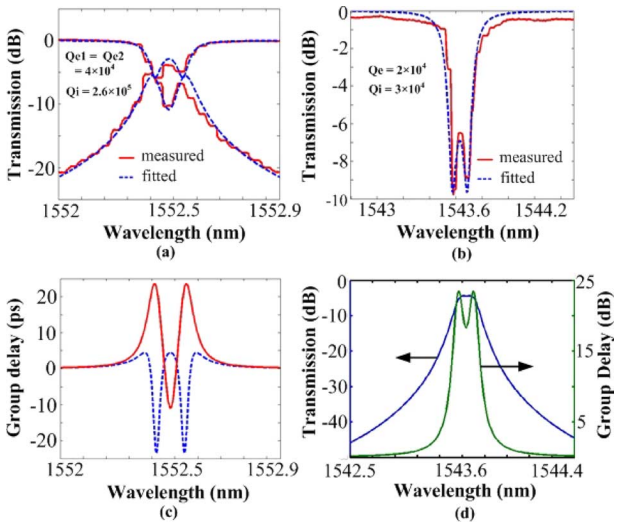

Fig. 9. Transmission spectra for the (a) double-waveguide and (b) single-waveguide coupled resonators. The red solid curves represent the measured transmission spectra and the blue dashed curves are the fitted ones. Group delay for the through channel (blue dashed curve) and drop channel (red solid curve) of the double-waveguide coupled resonator (c), and transmission (green curve) and group delay (blue curve) for the single-waveguide coupled resonator (d).

are 2.6×10^5 and 3.9×10^4, respectively, and Q_μ is 1.2×10^4, which corresponds to the under-coupling case. Using the quality factors derived from the spectra fitting and (4), we plot the group delays with respect to wavelength across the sub-resonances. For the through channel, Fig. 9(c) shows that maximal pulse advancement of $\sim$ 25 ps can be obtained at each split sub-resonance where a large negative group delay τ_t exists. For the drop channel, τ_d changes from positive to negative as the wavelength is tuned from each of the split sub-resonances to the central wavelength among them. The maximal delay and advancement values are $\sim$ 25 ps and $\sim$ 10 ps, respectively.

For the single-waveguide coupled resonator, spectral response is measured at the through port and fitted based on (5) to obtain the coupling Q_e, intrinsic Q_i, and mutual-coupling Q_μ, which are 2×10^4, 3×10^4 and 1.1×10^4, respectively, as shown in Fig. 9(b). Resonance splitting is obvious, proving the existence of the backward WGM. To explore the group delay feature at the reflection port, we plot the group delays as functions of wavelength using the quality factors derived from the spectra fitting and (7). Normal dispersion is achieved with the maximal delay and tunable range being $\sim$ 23 ps and $\sim$ 5 ps, respectively, as shown in Fig. 9(d). The maximal delay and tunable range could be improved if the quality factors wound be increased. The transmission at the reflection port is also plot in Fig. 9(d) without spectral fitting in that the measured spectrum is influenced by the fiber Fresnel reflection, which will be analyzed in the following part. The agreement between the group delays obtained from formula fittings and the measured pulse delay/advancement values in the following experiments verifies the phase characteristics of the resonator systems in the theoretical analysis without direct phase measurement.

B. Experimental Setup and Results

In the experiments, we focus on the drop port of the double-waveguide coupled resonator and the reflection port of the single-waveguide coupled resonator since the group delays display some different features at these two ports according to the theoretical analysis.

1) Continuously-Tunable Slow- to Fast Light: We use a return-to-zero (RZ) pulse train as a probe signal to experimentally demonstrate the pulse delay and advancement. The schematic diagram of the experimental setup is depicted in Fig. 10. The RZ pulse train with a duty cycle of 50% is generated by two cascaded Mach-Zehnder modulators (MZMs). The first MZM is driven by a 5-Gb/s pseudo-random bit sequence (PRBS) signal of 2^7-1 pattern length, and the second one is used as a pulse carver driven by a sinusoidal signal with the same rate as the data. The full width at half maximum (FWHM) of the signal pulse is 100 ps. An erbium-doped fiber amplifier (EDFA) is used to boost the generated probe signal followed by a tunable band-pass filter (BPF) with a bandwidth of 1.6 nm to reduce the ASE noise. A polarization controller is inserted before the resonator system to make sure that the input probe signal is in TE mode. The output pulse train is amplified by two-stage EDFAs and the noise is suppressed using another BPF. A variable optical attenuator (VOA) is used to make sure that the peak power of the advanced pulses is approximately equal to the delayed ones. Their temporal waveforms are taken with an oscilloscope.

We tune the wavelength of CW light to measure the pulse delay and advancement. As shown in Fig. 11, points A, B, C, and D correspond to four different wavelengths around the split resonances. First, we set the signal wavelength off resonance (point A) and take the corresponding pulse waveform (curve A), shown in Fig. 12(a). When the wavelength is tuned to one of the split resonances (point B), the pulse is delayed by $\sim$ 36 ps [Fig. 12(a), curve B]. When the signal wavelength sits between split resonances (point C), we observe that the pulse is advanced by $\sim$ 12 ps [Fig. 12(a), curve C]. Similarly, when the wavelength is tuned to another split resonance (point D), pulse delay is also obtained [Fig. 12(a), curve D]. To demonstrate continuous tuning by thermal control, a control light of 1543.21 nm is amplified by a high power EDFA followed by a VOA to adjust the power. Through a 3-dB coupler, it is fed to the resonator system together with the RZ signal pulses. Initially, the control power is attenuated to ~ -30 dBm and the wavelength of probe signal sits in the middle of two split resonances. The corresponding pulse waveform (curve A) is shown in Fig. 12(b). When the control power increases to 8.4 dBm, the resonances are red shifted due to the thermal effect [14]. The RZ signal then shifts towards the left split resonance, which causes

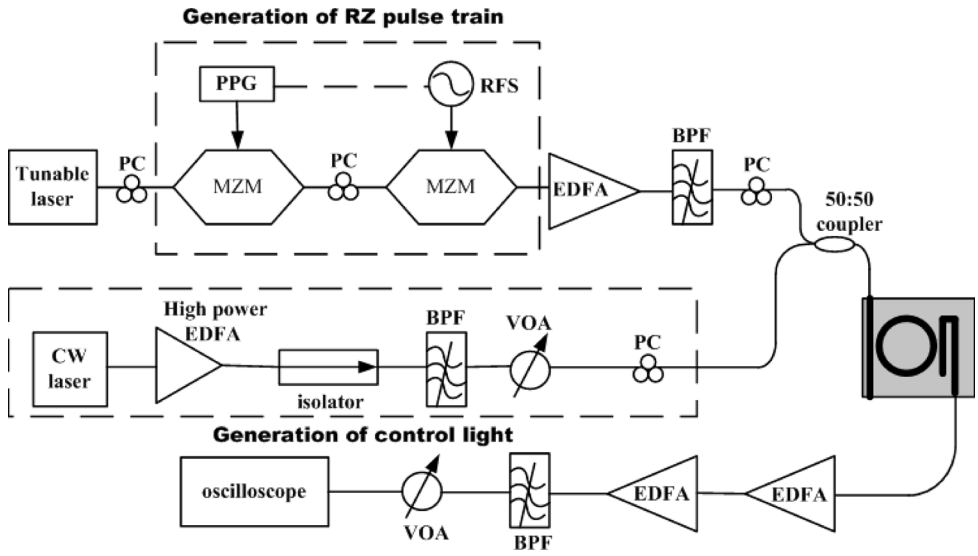

Fig. 10. Experimental setup in the optically tunable pulse delay and advancement demonstration using a double-waveguide coupled resonator.

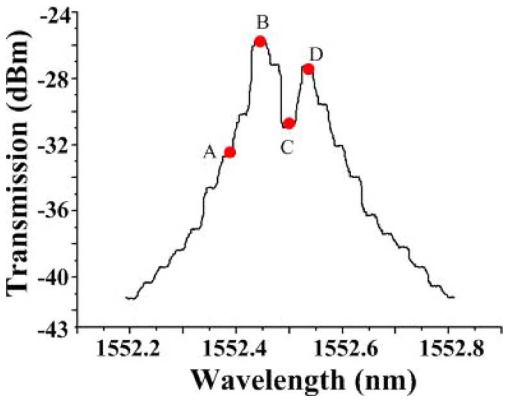

Fig. 11. Measured transmission spectrum in the drop channel of the double-waveguide coupled resonator.

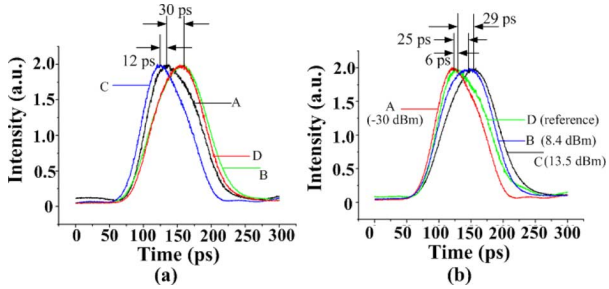

Fig. 12. Temporal waveforms of the RZ pulses with signal-wavelength detuning (a), and control-light thermal tuning (b), respectively.

a delay of ~ 25 ps [Fig. 12(b), curve B]. Pulse delay further increases [Fig. 12(b), curve C], when the control power goes up to 13.5 dBm, making the wavelength of the RZ signal closer to the left split resonance. Comparing with the reference pulse, one can observe that pulse propagation is continuously tuned from advancement ($\sim$ 6 ps) to delay ($\sim$ 29 ps). The tunable range would be extended if the control power further increases. There are two factors contributing to the RZ pulse distortion: 1) the edges of the RZ pulses contain most of the high frequency components, which experience more loss through the resonance filter; 2) it has been known that the group velocity dispersion at the resonance is zero [22], and the third-order dispersion plays an important role in the asymmetry of filtered pulses as one of their edges is steepened [27], [28]. Therefore, the resonator filter mainly changes the shape of pulse edges, but less on the peak. It should be noted that the temporal waveforms are smoothed using the average mode of the oscilloscope to evaluate the delay time more accurately.

2) Tunable Slow Light at the Reflection Port: Fig. 13 shows the experimental setup for the demonstration of pulse delay at the input/reflection port of a single-waveguide coupled resonator. The probe signal is an RZ pulse train, which is generated using the same approach as the last experiment. We use an optical circulator to perform the function of feeding the RZ pulses as well as allowing the reflected signals to pass through. Through an optical coupler, 95 percent of the output signal is amplified by an EDFA and taken by the oscilloscope after being filtered by a BPF and attenuated by a VOA. In addition, a power meter is used to record the variation of the output signal power. Initially, the transmission spectrum is measured at the reflection port, as shown in Fig. 14(a).

To illustrate the pulse delay measurement, we analyze the output signals from reflection port, which can be given by

$$S_o = A_1 S(t) + A_2 S(t - \Delta T) + A_3 S(t - T_g) \qquad (8)$$

where $\mathrm{A_1S(t)}$ is the signal caused by fiber Fresnel reflection, $\mathrm{A_2S(t-\Delta T)}$ is the signal reflected by the gold grating. $\Delta \mathrm{T}$ is the time light travelling in the spacing between the fiber facet and the grating. $\mathrm{A_3S(t-T_g)}$ represents the output backward WGM and $\mathrm{T_g}$ is the dispersion induced group delay. When the signal wavelength is off resonance, no backward WGM exists, i.e., $A_3 \approx 0$. The residual power reflected by the gold grating at the end of the straight waveguide is comparable with that caused

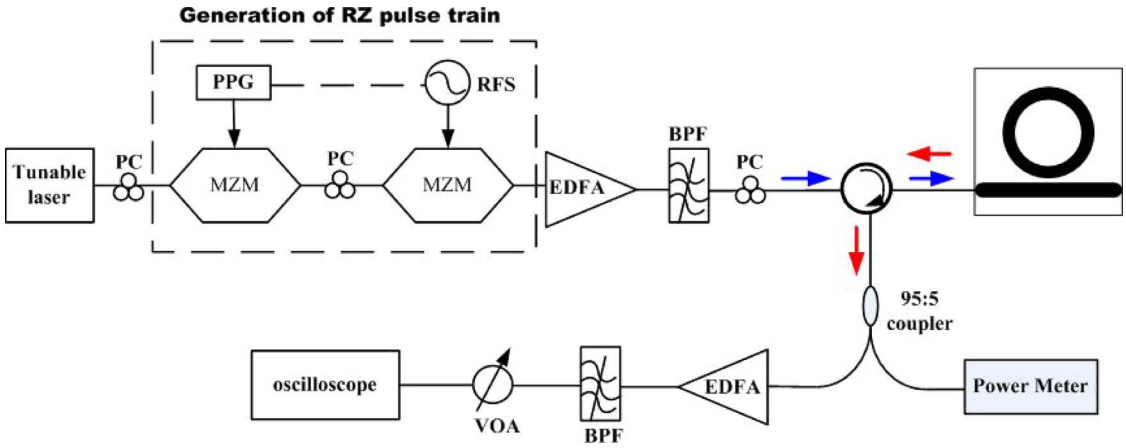

Fig. 13. Experimental setup in the optically tunable pulse delay demonstration using a single-waveguide coupled resonator.

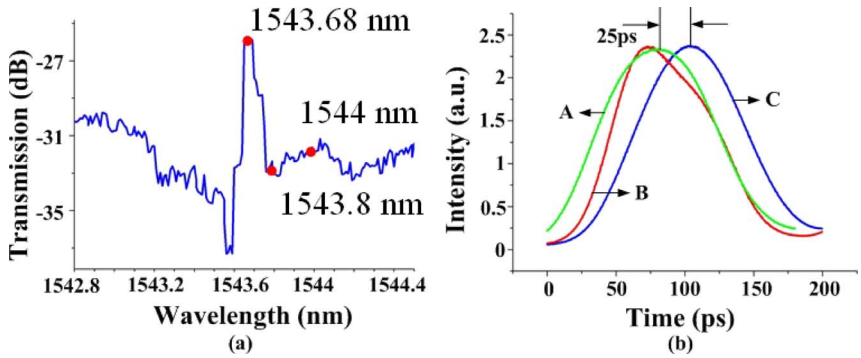

Fig. 14. (a) Measured transmission spectra of the reflection port and (b) temporal waveforms of the RZ pulses with signal-wavelength detuning.

by the Fresnel reflection, i.e., $A_1 \approx A_2$. Therefore, destructive and constructive interferences take place. Since the fiber facet is very close to the grating, ΔT is negligible and $S_0 = 2A_1S(t)$ can be approximately obtained. When the signal wavelength is on resonance, the transmission is ~ -5 dB, as shown in Fig. 9(d). Since the fiber Fresnel reflectivity is $\sim 0.25\%$, the optical power that is directly reflected by the fiber facet is approximately 26 dB lower than the input optical power, implying that the Fresnel reflection is ~ 4 dB lower than the output backward WGM considering the additional fiber-to-fiber loss of ~ 17 dB. Thus, the influence of the Fresnel reflection is negligible, i.e., $A_3 \gg A_1 + A_2$ and $S_0 \approx A_3S(t - T_g)$. Therefore, pulse delay can be evaluated by comparing the temporal waveform when the signal on resonance with that off resonance, even though there is some minor signal distortion.

As shown in Fig. 14(a), we firstly set the signal wavelength off resonance (1544 nm) and take the corresponding pulse waveform [Fig. 14(b), curve A]. When the wavelength is tuned to 1543.8 nm, the pulse exhibits some distortion due to the filtering effect [Fig. 14(b), curve B]. Further blue-shifting the signal wavelength induces continuously delay of the pulse and maximal delay time of $\sim$ 25 ps [Fig. 14(b), curve C], is obtained at 1543.68 nm, which is the resonance wavelength as shown in Fig. 9(b). It is well proved that pulse delay can be achieved at the reflection port of single-waveguide coupled resonators.

V. Conclusion

We numerically study and experimentally demonstrate pulse propagation in both double-waveguide and single-waveguide coupled resonators with mutual mode coupling. For the double-waveguide coupled resonators, theoretical analysis illustrates that tunable slow light can be achieved in the add channel with minor transmission variation. Experimentally, continuously tunable fast and slow light is demonstrated in the drop channel by thermally shifting the split resonances, and the observed maximal pulse delay and advancement are $\sim$ 29 ps and $\sim$ 6 ps, respectively. For the single-waveguide coupled resonators, slow light is observed at the reflection port with maximal pulse delay of $\sim$ 25 ps. In spite of the small tunable range, continuous tunability from slow to fast light in the resonator systems can still find some practical applications, such as continuously-controllable OTDM system [29] and synchronization of multiple data channels [30].

References

[1] J. Bowers, E. Burmeister, and D. Blumenthal, "Optical buffering and switching for optical packet switching," presented at the Photon. Switching Conf., Crete, Greece, 2006, O 16.1.

[2] R. Luijten, C. Minkenberg, R. Hemenway, M. Sauer, and R. Grzybowski, "Viable opto-electHPCinterconnect fabrics," in *Proc. ACM/IEEE SC2005 Supercomput. Conf.*, Seattle, WA, pp. 8–16.

[3] E. Parra and J. R. Lowell, "Toward applications of slow light technology," *Opt. Photon. News*, vol. 18, pp. 40–45, Nov. 2007.

[4] K. Y. Song, M. G. Herráez, and L. Thévenaz, "Gain-assisted pulse advancement using single and double Brillouin gain peaks in optical fibers," *Opt. Exp.*, vol. 13, no. 24, pp. 9758–9765, Nov. 2005.
[5] B. Pesala, Z. Chen, A. V. Uskov, and C. Chang-Hasnain, "Electrically tunable fast light at THz bandwidth using cascaded semiconductor optical amplifiers," *Opt. Exp.*, vol. 14, no. 24, pp. 15863–15867, Nov. 2006.
[6] M. A. I. Talukder, Y. Amagishi, and M. Tomita, "Superluminal to subluminal transition in the pulse propagation in a resonant absorbing medium," *Phys. Rev. Lett.*, vol. 86, no. 16, pp. 3546–3549, Apr. 2001.
[7] M. M. Kash *et al.*, "Nonlinear magneto-optics and reduced group velocity of light in atomic vapor with slow ground state relaxation," *Phys. Rev. Lett.*, vol. 82, no. 26, pp. 5229–5232, Jun. 1999.
[8] K. Totsuka and M. Tomita, "Slow and fast light in a microsphere-optical fiber system," *J. Opt. Soc. Amer. B*, vol. 23, no. 10, pp. 2194–2199, Oct. 2006.
[9] F. Xia, L. Sekaric, and Y. Vlasov, "Utracompact optical buffers on a silicon chip," *Nat. Photon.*, vol. 1, pp. 65–71, Jan. 2007.
[10] Q. Li, Z. Zhang, J. Wang, M. Qiu, and Y. Su, "Fast light in silicon ring resonator with resonance-splitting," *Opt. Exp.*, vol. 17, no. 2, pp. 933–940, Jan. 2009.
[11] S. Manipatruni, P. Dong, Q. Xu, and M. Lipson, "Tunable superluminal propagation on a silicon microchip," *Opt. Lett.*, vol. 33, no. 24, pp. 2928–2930, Dec. 2008.
[12] T. Wang, F. Liu, T. Ye, Z. Zhang, J. Wang, Y. Tian, M. Qiu, and Y. Su, "Continuously-tunable slow and fast light using silicon microring add-drop filter with mutual mode coupling," presented at the OFC, 2009, OWC4.
[13] T. J. Kippenberg, S. M. Spillane, and K. J. Vahala, "Mode coupling in traveling-wave resonators," *Opt. Lett.*, vol. 27, no. 19, pp. 1669–1671, Oct. 2002.
[14] Q. Xu and M. Lipson, "Carrier-induced optical bistability in silicon ring resonators," *Opt. Lett.*, vol. 31, no. 3, pp. 341–343, Feb. 2006.
[15] G. Priem *et al.*, "Optical bistability and pulsating behaviour in silicon-on-insulator ring resonator structures," *Opt. Exp.*, vol. 13, pp. 9623–9628, 2005.
[16] Q. Li, Z. Zhang, F. Liu, M. Qiu, and Y. Su, "Dense wavelength conversion and multicasting in a resonance-split silicon microring," *Appl. Phys. Lett.*, vol. 93, p. 081113, Aug. 2008.
[17] F. Liu, Q. Li, Z. Zhang, M. Qiu, and Y. Su, "Ultra-compact mode-split silicon microring resonator for format conversion from NRZ to FSK," in *Proc. SPIE*, 2008, vol. 7135, p. 713537.
[18] Q. Chang, Q. Li, Z. Zhang, M. Qiu, and Y. Su, "Micrometer-scale optical up-converter using a resonance-split silicon microring resonator in radio over fiber systems," presented at the OFC, 2009, JWA48.
[19] Z. Zhang, M. Dainese, L. Wosinski, and M. Qiu, "Resonance-splitting and enhanced notch depth in SOI ring resonators with mutual mode coupling," *Opt. Exp.*, vol. 16, no. 7, pp. 4621–4630, Mar. 2008.
[20] C. Manolatou, M. J. Khan, S. Fan, P. R. Villeneuve, H. A. Haus, and J. D. Joannopoulos, "Coupling of modes analysis of resonant channel add-drop filters," *IEEE J. Quant. Electron.*, vol. 35, pp. 1322–1331, Sep. 1999.
[21] G. Lenz, B. J. Eggleton, C. K. Madsen, and R. E. Slusher, "Optical delay lines based on optical filters," *IEEE J. Quant. Electron.*, vol. 37, pp. 525–532, Apr. 2001.
[22] J. E. Heebner and R. W. Boyd, "'Slow' and 'fast' light in resonator-coupled waveguides," *J. Mod. Opt.*, vol. 49, no. 14/15, pp. 2629–2636, Mar. 2002.
[23] O. Schwelb, "Transmission, group delay and dispersion in single-ring optical resonators and add/drop filters – A tutorial overview," *J. Lightw. Technol.*, vol. 22, pp. 1380–1394, May 2004.
[24] Q. Chang, Q. Li, Z. Zhang, M. Qiu, T. Ye, and Y. Su, "A tunable broadband photonic Rf phase shifter based on a silicon microring resonator," *IEEE Photon. Technol. Lett.*, vol. 21, pp. 60–62, Jan. 2009.
[25] F. Liu, Q. Li, Z. Zhang, M. Qiu, and Y. Su, "Optically tunable delay line in silicon microring resonator based on thermal nonlinear effect," *IEEE J. Sel. Topics Quant. Electron.*, vol. 14, no. 3, pp. 706–712, May/Jun. 2008.
[26] S. Scheerlinck, J. Schrauwen, F. Van Laere, D. Taillaert, D. Van Thourhout, and R. Baets, "Efficient, broadband and compact metal grating couplers for silicon-on-insulator waveguides," *Opt. Exp.*, vol. 15, no. 15, pp. 9639–9644, 2007.
[27] Y. Wang, W. Hu, Y. Su, Z. Zheng, L. Leng, X. Tian, and Y. Jin, "Performance study of 40-Gb/s RZ signals through cascaded thin-film filters with large dispersion slope," *Opt. Exp.*, vol. 13, no. 6, pp. 2176–2181, Mar. 2005.
[28] G. P. Agrawal, *Nonlinear Fiber Optics*, 2nd ed. New York: Academic, 1995, ch. 3.
[29] B. Zhang, L. Zhang, L.-S. Yan, I. Fazal1, J.-Y. Yang, and A. E. Willner, "Continuously-tunable, bit-rate variable OTDM using broadband SBS slow-light delay line," *Opt. Exp.*, vol. 15, pp. 8317–8322, Jun. 2007.
[30] B. Zhang, L. Zhang, L.-S. Yan, I. Fazal1, J.-Y. Yang, and A. E. Willner, "A single slow-light element for independent delay control and synchronization on multiple Gb/s data channels," *IEEE Photon. Technol. Lett.*, vol. 19, pp. 1081–1083, 2007.

Tao Wang (S'08) received the B.S. degree in electronic engineering from the Department of Electronic Engineering, Shandong University, China, in 2004, and M.S. degree from the graduate school of the Chinese Academy of Sciences, China, in 2007. He is currently pursuing the Ph.D. degree at Shanghai Jiao Tong University, Shanghai, China.

His current research interests include microwave photonics and information processing in silicon waveguides.

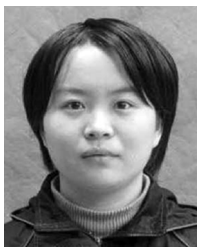

Fangfei Liu (S'07) received the B.S. degree in electronic engineering in 2007 from the Department of Electronic Engineering, Shanghai Jiao Tong University, Shanghai, China, where she is currently a graduate student.

Her current research interests include advanced modulation formats for high-speed optical communication systems, nonlinear optics in waveguides and fibers, and optical signal processing.

Jing Wang received the B.S. and M.S. degrees in sciences of materials from Xiamen University, China, in 2004 and 2007. She is currently pursuing the Ph.D. degree in the Microelectronics and Applied Physics Department, Royal Institute of Technology (KTH), Sweden.

Her research interests are silicon-based devices, including designs, fabrications, and characterizations.

Yue Tian, photograph and biography not available at the time of publication.

Ziyang Zhang received the B.S. degree in optical engineering from Zhejiang University, Hangzhou, China, in 2003, and the M.S. and Ph.D. degrees in photonics from the Department of Microelectronics and Applied Physics, Royal Institute of Technology (KTH), Stockholm, Sweden, in 2004 and 2008, respectively.

He is currently a postdoctorate researcher at the Heinrich-Hertz Institute, Berlin, Germany. His research area covers the design, fabrication, and characterization of silicon/polymer based photonic devices.

Tong Ye received the B.S. and M.S. degrees from the University of Electronic Science and Technology of China, Chengdu, in 1998 and 2001, respectively, and the Ph.D. degree in electronics engineering from Shanghai Jiao Tong University, Shanghai, China, in 2005.

He was with the Chinese University of Hong Kong for one and half years before he joined the Shanghai Jiao Tong University as a Lecturer in 2006. His research interests mainly include high-speed transmission, optical signal processing, and physical layer optical networking.

Min Qiu (M'99) received the B.Sc. and Ph.D. degrees from Zhejiang University, Hangzhou, China, in 1995 and 1999, respectively, and a second Ph.D. degree in electromagnetic theory from the Royal Institute of Technology (KTH), Stockholm, Sweden, in 2001.

In 2001, he joined the Department of Microelectronics and Applied Physics, KTH, where he is currently an Associate Professor. He also holds a Senior Researcher Fellowship from the Swedish Research Council, Stockholm, Sweden. He is the author or coauthor of more than 80 international refereed journal papers, and more than 60 conference contributions. His current research interests include optical metamaterials, photonic crystals, plasmonic optics, and integrated optical circuits.

Dr. Qiu is a member of the Optical Society of America and the European Optical Society. He was the recipient of the Individual Grant of Future Research Leader (INGVAR) from the Swedish Foundation for Strategic Research (SSF) in 2004.

Yikai Su (A'95–M'95–S'97–M'01–SM'07) received the B.S. degree from the Hefei University of Technology, Hefei, China, in 1991, the M.S. degree from the Beijing University of Aeronautics and Astronautics, Beijing, China, in 1994, and the Ph.D. degree in electronics engineering from Northwestern University, Evanston, IL, in 2001.

He was with Crawford Hill Laboratory of Bell Laboratories for three years before he joined the Shanghai Jiao Tong University, Shanghai, China, as a Full Professor in 2004. He became the Associate Department Chair of Electronic Engineering in 2006. He is the author or coauthor of more than 170 papers published in prestigious international journals and conferences, including 40 IEEE PHOTONICS TECHNOLOGY LETTERS papers, ~30 invited conference presentations, and eight postdeadline papers. He holds four U.S. patents with over ten U.S. or Chinese patents pending. His current research interests include ultrahigh-speed transmission and modulation formats, optical signal processing, and enabling devices and modules for information processing.

Prof. Su is a member of the Optical Society of America. He serves as a Co-Chair of the Workshop on Optical Transmission and Equalization (WOTE) 2005, the ChinaCom 2007 Symposium, the IEEE/OSA AOE 2007 Slow Light Workshop, Asia Pacific Optical Communications (APOC) 2008 SC3, and a Technical Committee Member of the Opto-Electronics and Communications Conference (OECC) 2008, the Conference on Laser and Electro-Optics (CLEO) Pacific Rim (PR) 2007, the IEEE Lasers and Electro-Optics Society (LEOS) Summer Topical Meeting 2007 on ultrahigh-speed transmission, the IEEE Lasers and Electro-Optics Society (LEOS) 2005–2007, the BroadNets 2006, the Asia-Pacific Optical Communications (APOC) Conference 2005, and the International Conference on Optical Communications and Networks (ICOCN) 2004. He is a Topical Editor of Optics Letters, Guest Editor of IEEE JSTQE on "Nonlinear Optical Signal Processing" May/June issue of 2008, and Feature Editor of Applied Optics on the special issue of AOE 2008.